Relativistic extension of the Troullier-Martins scheme: Accurate pseudopotentials for transition-metal elements

E. Engel and A. Höck
Institut für Theoretische Physik, Universität Frankfurt, D-60054 Frankfurt/Main, Germany

S. Varga
Department of Experimental Physics, Chalmers University of Technology, S-41296 Göteborg, Sweden
(Received 18 August 2000; revised manuscript received 13 December 2000; published 13 March 2001)

A fully relativistic extension of the pseudopotential construction scheme by Troullier and Martins [Phys. Rev. B **43**, 1993 (1991)] is presented. The resulting pseudopotentials are applied to a number of transition and noble metal compounds. For an unambiguous discussion of the relativistic contributions the convergence of the pseudopotential results with the size of the valence space is carefully investigated. Our results show that, for a fully quantitative comparison with experiment, pseudopotential calculations for transition and noble metal elements should treat the semicore *s* states dynamically, rather than via nonlinear core corrections. Using such a large valence space, very good agreement of the calculated spectroscopic parameters with the corresponding all-electron data is obtained. Reliable predictions seem to be possible, even for very critical systems like FeO. The relativistic corrections are found to be significant for all $3d$ transition metal compounds considered.

DOI: 10.1103/PhysRevB.63.125121 PACS number(s): 71.15.Dx, 71.15.Mb, 31.10.+z

I. INTRODUCTION

A substantial fraction of present-day electronic structure calculations, covering such a variety of topics as magnetic materials (see, e.g., Ref. 1), vacancies and impurities,[2] quasi-crystals,[3] surfaces,[4] clusters[5] and theoretical biophysics,[6] is based on the pseudopotential (PP) approach. Among the various PP schemes the concept of normconserving PPs[7] in the Troullier-Martins (TM) form[8] appears to be the most widely used. Both the original and the TM variant of normconserving PPs are formulated within the framework of density functional theory[9] (DFT). While the original approach starts with a fully relativistic all-electron (AE) treatment of the atom and its actual PP construction procedure is independent of the handling of relativity, the PP construction of TM explicitly makes use of the nonrelativistic Kohn-Sham (KS) equations. However, relativistic effects already become visible in the spectroscopic constants of molecules containing $3d$ elements (see, e.g., Refs. 10–12 for the Copper dimer and Sec. IV) and can definitively not be neglected for heavy elements.[13] In practical implementations of the TM scheme relativistic effects are thus sometimes taken into account in the AE calculation on the scalar-relativistic level, while still using the nonrelativistic form of the actual PP generation.[14] Here we present a fully relativistic extension of the TM approach which explicitly includes spin-orbit coupling in the PP construction. This not only resolves the inconsistency of the semi-relativistic procedure, but also provides the input for DFT calculations on the basis of TM-PPs without neglect of spin-orbit effects (in analogy to spin-orbit coupled energy adjusted PPs[15]).

In order to generate particularly smooth pseudo-orbitals (POs) the TM procedure augments the AE valence orbitals in the valence region by nodeless continuations into the core region in such a way that the POs and their first four derivatives are continuous. The corresponding screened PPs for the individual valence states are then obtained from these POs via the nonrelativistic KS equations. The latter step must be modified as soon as the AE orbitals result from the solution of the relativistic KS equations. Although in the core region the POs experience much weaker total potentials (i.e., the corresponding PPs) than the AE orbitals, the depths of these potentials are nevertheless often too large to allow for a complete neglect of relativistic corrections. In such cases, use of the nonrelativistic KS equation for the extraction of the screened PP from the PO introduces a sizable error. This error becomes visible as soon as the Dirac equation is solved for the resulting PP. The solution deviates from the AE spinor even in the valence region, as the inconsistency in the core regime is propagated into the valence regime by the integration of the differential equation. In spite of its weakly relativistic nature, this inconsistency is not only a formal problem, but rather shows up in a practical, numerical sense. The TM scheme thus has to be reformulated within a fully relativistic framework (Sec. II).

The resulting PPs are applied to a number of prototype molecules. In order to establish the reliability of the relativistic TM scheme, we consider three noble metal compounds, Cu_2, Au_2 and AuH. These diatomic systems are particularly suitable for an unambiguous analysis of the performance of the relativistic PPs, as very accurate AE reference data are available, both for the nonrelativistic and the relativistic case[10–12,16] (especially for Cu_2).

On this basis we focus on $3d$ transition metal elements. It is well known that for these elements the $3s$ and $3p$ semicore states cannot be completely neglected in a realistic description of compounds or the bulk.[1,17–22] Although these states are energetically well separated from the $3d$ and $4s$ valence electrons, the spatial overlap between the $3s$-, $3p$-, and $3d$-densities is large. This overlap shows up both in the total energy and in the effective single-particle equations of DFT via the exchange-correlation (xc) energy functional $E_{\mathrm{xc}}[n]$ and the corresponding xc-potential, $v_{\mathrm{xc}}[n]$

$=\delta E_{\rm xc}[n]/\delta n$, as $E_{\rm xc}[n]$ is a nonlinear functional of the density n. The neglect of the core density n_c in the total (spin-) density is particularly critical for magnetic systems, as, in this case, the balance between the spin-up and spin-down potentials is affected. For transition metal elements the semicore states are usually taken into account by inclusion of nonlinear core corrections (nlccs).[17] In fact, the nonlinearity of $E_{xc}[n]$ requires the application of nlccs also for many other atoms, like the alkalis (for a detailed discussion see Refs. 22 and 23). It has been shown that in this way good agreement with AE results for bulk iron, cobalt, and nickel can be obtained.[18,19] The situation is less clear for transition metal clusters (compare Refs. 24, 25, and 30) and has not been examined at all for transition metal oxides.[26] As an alternative to their representation by nlccs, one can treat the semicore electrons dynamically,[21] i.e., extend the valence space by the semicore states.[27]

As a prerequisite for a reliable discussion of relativistic effects in transition metal compounds, we carefully analyze the convergence of the PP results with respect to the size of the valence space (in Sec. IV A—some technical issues concerning the construction of the PPs are discussed in Sec. III). In particular, we investigate to what extent the representation of the semicore electrons by nlccs can substitute their explicit dynamic treatment. For this question FeO provides a very critical testing ground as one finds three states that are energetically competing for being the ground state, and even rather elaborate multi-configuration Hartree-Fock calculations[28] do not correctly reproduce the experimental ground state.[29,30] It represents a serious challenge for any PP-scheme to reproduce the energetic ordering of the three states, as predicted by AE-calculations with the same xc-functional (which need not necessarily be identical with the experimental ordering). With the converged PP results we then investigate the importance of relativity (in Sec. IV B).

For this conceptual study we utilize the local density approximation (LDA)[31] for $E_{\rm xc}[n]$. It must be emphasized, however, that the complete approach can be directly transferred to semilocal functionals (like the generalized gradient approximation: GGA) or fully nonlocal xc functionals (like the exact exchange implemented via the optimized potential method—see, e.g., Refs. 32 and 33).

II. THEORY

A. Relativistic extension of Troullier-Martins scheme

The general form of the semilocal PPs usually applied in the context of DFT is[7]

$$\langle \boldsymbol{r}|\hat{v}_{\rm ps}|\boldsymbol{r}'\rangle = v_{\rm loc}(r)\,\delta^{(3)}(\boldsymbol{r}-\boldsymbol{r}') + \frac{\delta(r-r')}{r^2} \times \sum_{l=0}^{l_{\max}} \delta v_{sl,l}(r) \sum_{m=-l}^{l} Y_{lm}(\Omega) Y_{lm}^{*}(\Omega'), \quad (1)$$

$$\delta v_{{\rm sl},l}(r) = \sum_{j=l\pm 1/2} \frac{2j+1}{4l+2}[v_{{\rm ps},lj}(r) - v_{\rm loc}(r)], \quad (2)$$

i.e., for each angular momentum $l \leqslant l_{\max}$ present among the valence levels of the atom of interest, a separate radial PP is used to represent the atom's ionic core in electronic structure calculations for molecules or solids. While the latter calculations are typically based on the framework of nonrelativistic spin-density functional theory,[9] Eq. (1) already indicates that, in general, a relativistic treatment of the atom is necessary. Consequently, a j average is required for the transition from the relativistic, lj-dependent PPs $v_{{\rm ps},lj}$, resulting directly from a fully relativistic PP construction scheme, to the purely l-dependent PPs usually applied in the poly-atomic calculations. On the other hand, without j averaging, the $v_{ps,lj}$ can be used as input to spin-orbit coupled PP calculations on the basis of norm-conserving PPs. As usual, a multiplicative part $v_{\rm loc}$ of the total PP has been extracted from the individual components in Eq. (1). $v_{\rm loc}$ is chosen so that the resulting $\delta v_{{\rm ps},l}$ are short-ranged. For the calculations of Sec. V always one of the j averaged $v_{{\rm ps},lj}$ is used for $v_{\rm loc}$.[34]

For the construction of the individual $v_{ps,lj}$ one starts with an AE calculation for a suitably chosen atomic valence configuration (utilizing a spherical average). In the context of the LDA, often excited and/or ionized configurations are utilized in order to stabilize unoccupied states,[7] which may not even be bound by the ground state KS potential. However, in this contribution, we restrict ourselves to using the ground state configuration only.[35]

In the most general situation, the atomic AE calculation requires the solution of the radial KS equations of relativistic DFT (for the notation see Ref. 36),

$$c\left(\partial_r + \frac{\kappa}{r}\right) a_{nlj}(r) = [2mc^2 - v_s(r) + \epsilon_{nlj}] b_{nlj}(r), \quad (3)$$

$$c\left(\partial_r - \frac{\kappa}{r}\right) b_{nlj}(r) = [v_s(r) - \epsilon_{nlj}] a_{nlj}(r), \quad (4)$$

where

$$v_s(r) = -\frac{Ze^2}{r} + v_H(r) + v_{xc}(r), \quad (5)$$

$$v_H([n];r) = 4\pi e^2 \left\{ \frac{1}{r}\int_0^r x^2 dx\, n(x) + \int_r^\infty x dx\, n(x) \right\}, \quad (6)$$

$$v_{\rm xc}([n];r) = \frac{\delta E_{\rm xc}[n]}{\delta n(\boldsymbol{r})}, \quad (7)$$

$$n(r) = \sum_{nlj} \Theta_{nlj} \frac{a_{nlj}(r)^2 + b_{nlj}(r)^2}{4\pi r^2}, \quad (8)$$

with Θ_{nlj} denoting the occupation of each nlj subshell ($\kappa = -2(j-l)(j+1/2)$—we use the standard form of the spherical spinors as given by Rose[37]). Self-consistent solution of Eqs. (3)–(8) provides the total AE potential v_s as well as the radial AE orbitals a_{nlj} and b_{nlj} and the eigenvalues ϵ_{nlj}.

On the basis of these solutions one has to choose a set of cutoff radii $r_{c,l}$ for the individual valence states, thus sepa-

rating the (outer) valence from the (inner) core region. While the pseudo-orbital (PO) is required to be identical with the AE orbital for $r>r_{c,l}$, one has to make a suitable ansatz for the PO inside the core region. This step is somewhat complicated by the fact that, in the relativistic situation, each orbital consists of two components. Clearly, for all valence and semicore states a_{nlj} dominates over b_{nlj}, so that the primary quantity for the PP construction is the large component. The standard TM scheme[8] thus suggests the ansatz

$$a_{\mathrm{ps},lj}(r)=\begin{cases} a_{nlj}(r) & \text{for } r>r_{c,l} \\ r^{l+1}\exp[p(r)] & \text{for } r\leqslant r_{c,l}, \end{cases} \tag{9}$$

$$p(r)=\sum_{i=0}^{6} c_{2i}r^{2i}, \tag{10}$$

for the large component of the PO.[38] In the standard TM procedure the corresponding screened PP $v^{\mathrm{sc}}_{\mathrm{ps},lj}$ (which is the total potential of which $a_{\mathrm{ps},lj}$ is an eigenstate) follows immediately from the nonrelativistic KS equation,[8]

$$v^{\mathrm{sc,nr}}_{\mathrm{ps},lj}=\begin{cases} v_s & \text{for } r>r_{c,l}, \\ \epsilon_{nlj}+\dfrac{l+1}{r}\dfrac{p'}{m}+\dfrac{p''+(p')^2}{2m} & \text{for } r\leqslant r_{c,l}. \end{cases} \tag{11}$$

Equations. (9)–(11) would be consistent if a_{nlj} and v_s were related via the nonrelativistic KS equations. In the present, more general situation, however, the AE orbitals are solutions of the Dirac-type equations (3) and (4). Thus, for a continuous PO of the form (9), (10), the PP (11) is discontinuous at $r_{c,l}$, in obvious contradiction to the TM concept. In fact, in the complete core region the PO (9), (10) (together with the associated small component) does not really solve Eqs. (3) and (4) for the PP (11).

To analyze this problem in more detail, it is most convenient to combine Eqs. (3) and (4) to a second-order differential equation for the large component,

$$\frac{1}{2m}\left(\frac{1}{1-\Delta}\right)\left[\partial_r^2-\frac{l(l+1)}{r^2}+\frac{(\partial_r\Delta)}{1-\Delta}\left(\partial_r+\frac{\kappa}{r}\right)\right]a(r) =(v(r)-\epsilon)a(r), \tag{12}$$

where

$$\Delta(r)=\frac{v(r)-\epsilon}{2mc^2} \tag{13}$$

and all quantum numbers and indices have been dropped for brevity. Equation (12) not only applies for the AE solution, but also establishes the connection between consistent relativistic POs and PPs in the core region. As is obvious from Eq. (12), the relevant ratio that characterizes the difference between the relativistic and nonrelativistic KS equations is Δ, so that the inconsistency between Eqs. (9) and (11) is of the order of $1/c^2$. In the standard range of $r_{c,l}$ (0.5–3.0 Bohr) Δ is of the order of 10^{-4}–10^{-3}. One may thus ask whether the inconsistency inherent in Eqs. (9)–(11) is of any practical relevance, given the fact that all quantities involved in Eqs. (9)–(11) are only known within some finite numerical accuracy.

A first answer to this question is provided by the following considerations: The POs not only serve as a vehicle in the construction of the screened PPs, they are also required for the elimination of the interaction among the valence electrons (and their spurious self-interaction, if present) from $v^{\mathrm{sc}}_{\mathrm{ps},lj}$. In the most simple case, linear unscreening is used for this purpose:

$$v_{\mathrm{ps},lj}(r)=v^{\mathrm{sc}}_{\mathrm{ps},lj}(r)-v_H([n_{\mathrm{ps}}];r)-v_{\mathrm{xc}}([n_{\mathrm{ps}}];r), \tag{14}$$

$$n_{\mathrm{ps}}(r)=\sum_{\mathrm{occ.val.orb.}}\Theta_{nlj}\frac{a_{\mathrm{ps},lj}(r)^2+b_{\mathrm{ps},lj}(r)^2}{4\pi r^2}. \tag{15}$$

(Note that the precise form of the unscreening is irrelevant for the arguments to follow.) In the unscreening procedure, one cannot simply ignore the existence of the small component by setting $b_{\mathrm{ps},lj}=0$, absorbing its norm contribution via

$$\int_0^{r_c}dr\,a(r)^2+\int_0^{\infty}dr\,b(r)^2=\int_0^{r_c}dr\,a_{\mathrm{ps}}(r)^2.$$

This would lead to an incomplete cancellation of the AE xc potential by $v_{\mathrm{xc}}([n_{\mathrm{ps}}];r)$ and also affect the charge balance of the system, and thus the net v_H (the charge represented by b_{nlj} in the valence regime is of the order of 10^{-5}–10^{-4} for most states, while its total norm contribution is larger by roughly one order of magnitude).

The most direct way to evaluate $b_{\mathrm{ps},lj}$ is the solution of Eqs. (3), (4) for the PP (11). However, due to the nonrelativistic form of (11) for $r<r_{c,l}$ the solutions of Eqs. (3), (4) do no longer have exactly the same eigenvalues as the AE states. For the size of this eigenvalue deviation, not only is $\Delta(r_{c,l})$ relevant, but rather the magnitude of Δ in the complete core region. For instance, for Cu the eigenvalue shift experienced by the $3d_{3/2}$ orbital amounts to 10 mHartree, reflecting the fact that for d states of transition or noble metals the ratio $(v_{\mathrm{ps}}-\epsilon)/(2mc^2)$ may become as large as 10^{-2} inside the core region. As a consequence, unscreening with the solutions of Eqs. (3), (4) for the PP (11) also leads to an incomplete cancellation of the interaction between the valence electrons, so that in the unscreened PP (14) the valence regime is affected by the size of Δ in the core region (see Sec. IV for a numerical example of the consequences of this effect for molecular results).

This problem can be circumvented by constructing the small component of the PO in an alternative way. Evaluation of b_{ps} by insertion of Eqs. (9) and (10) into Eq. (3),

$$b_{\mathrm{ps}}(r)=\begin{cases} b(r) & \text{for } r>r_c, \\ \dfrac{c[(l+1+\kappa)/r+p'(r)]a_{\mathrm{ps}}(r)}{2mc^2-v^{\mathrm{sc}}_{\mathrm{ps}}(r)+\epsilon} & \text{for } r\leqslant r_c, \end{cases} \tag{16}$$

guarantees that the resulting PO is identical with the AE orbital for $r>r_c$. Moreover, requiring proper normalization,

$$\int_0^{r_c} dr[a(r)^2+b(r)^2]=\int_0^{r_c} dr[a_{\rm ps}(r)^2+b_{\rm ps}(r)^2], \tag{17}$$

one is left with a minor charge redistribution in the core region. Equations (16) and (17) are equivalent to the approach taken in the scalar-relativistic PP scheme,[14] as in the latter, the small component is completely suppressed, allowing for a unique normalization of the large component. However, this construction of $b_{\rm ps}$ does not resolve the fundamental problem that the PO (9), (16) is not an eigenstate of the PP (11). While the j average (2) usually masks this problem, the basic inconsistency becomes immediately obvious in applications of the resulting unscreened PP to atoms. Self-consistent relativistic calculations with this PP do not yield the original AE levels as eigenstates.

To be consistent, the PP (11) therefore has to be augmented by some relativistic correction δv_{lj} for $r \leqslant r_{c,l}$,

$$v^{\rm sc}_{{\rm ps},lj}(r)=\begin{cases} v_s(r) & \text{for } r>r_{c,l}, \\ v^{\rm sc,nr}_{{\rm ps},lj}(r)+\delta v_{lj}(r) & \text{for } r\leqslant r_{c,l} \end{cases} \tag{18}$$

(note that this extension of the PP can equally well be used within the scalar-relativistic framework.) In contrast to its nonrelativistic limit, the nonlinear relation (12) does not directly allow to determine $v^{\rm sc}_{\rm ps}$ (or, alternatively, δv) for given $a(r)$, so that one has to resort to some approximation. In view of the size of Δ, a first-order weakly relativistic expansion of (12) offers itself,

$$\frac{1}{2m}\left[(1+\Delta)\left(\partial_r^2-\frac{l(l+1)}{r^2}\right)+\Delta'\left(\partial_r+\frac{\kappa}{r}\right)\right]a=(v-\epsilon)a. \tag{19}$$

Insertion of $v^{\rm sc}_{\rm ps}=v^{\rm sc,nr}_{\rm ps}+\delta v$ into Eq. (19) yields δv in terms of $v^{\rm sc,nr}_{\rm ps}$ and a,

$$\delta v=\frac{(v^{\rm sc,nr}_{\rm ps}-\epsilon)^2}{2mc^2}+\frac{(v^{\rm sc,nr}_{\rm ps})'}{4m^2c^2}\left(\frac{a'_{\rm ps}}{a_{\rm ps}}+\frac{\kappa}{r}\right). \tag{20}$$

Equations (11), (18), and (20) provide an excellent approximation to the potential satisfying the fully relativistic relations (3), (4) for a PO of the form (9), (10), (16). The remaining inconsistency of the order $1/c^4$ can no longer be resolved, given the limited numerical accuracy of the AE solution and all subsequent steps. Correspondingly, the eigenvalue shift discussed earlier is reduced to the order of 10 μHartree or less, and the POs generated by solution of Eqs. (3), (4) with the PP (11), (18), (20) are extremely close to the AE orbitals for $r>r_{c,l}$.

It remains to determine the coefficients c_{2i} in (10) in a relativistically consistent form. As in the nonrelativistic limit, one requires the continuity of $a_{{\rm ps},lj}$ and its first four derivatives at $r_{c,l}$ (and normalization of the PO). The actual implementation of these conditions, however, now makes use of the relativistic KS equation (12). The corresponding relations are explicitly given in the Appendix. Note, however, that in general, the relativistic corrections in Eqs. (A1)–(A5) are only of minor importance compared to those in Eq. (18), as $\Delta(r)$ is much smaller at $r=r_{c,l}$ than inside the core region.

TABLE I. Cutoff radii used in this work. Wherever different orbitals have been utilized to generate PPs for a given l both r_c are listed.

Atom	r_c [Bohr] s	p	d	$r_{\rm nlcc}$ [Bohr]
O	1.0	0.9	—	0.27
Cr	3: 0.8; 4: 2.2	3: 0.8; 4: 2.6	0.8	0.3
Mn	3: 0.81; 4: 2.53	3: 0.81; 4: 2.75	0.81	0.43
Fe	3: 0.8; 4: 2.2	3: 0.8; 4: 2.6	0.8	0.3
Co	3: 0.7; 4: 2.2	3: 0.7; 4: 2.6	0.7	0.3
Ni	3: 0.7; 4: 2.0	3: 0.7; 4: 2.5	0.7	0.25
Cu	3: 0.7; 4: 2.1	3: 0.7; 4: 2.5	0.6	0.25
Au	5: 0.85; 6: 2.2	5: 1.0; 6: 3.0	1.2	0.6

B. Nonlinear unscreening

The unscreening (14) implies a linearization of $v_{xc}[n]$ as far as the core-valence interaction is concerned. The nonlinearity of the xc functional can be taken into account by inclusion of nlccs,[17,27]

$$v^{\rm nlcc}_{{\rm ps,lj}}(r)=v^{\rm sc}_{{\rm ps,lj}}(r)-v_H([n_{\rm ps}];r)-v_{\rm xc}([n_{\rm ps}+n_c];r). \tag{21}$$

In order to end up with a sufficiently smooth $v^{\rm nlcc}_{{\rm ps},l}$, the AE core density n_c is usually modified for r smaller than some core-cutoff radius $r_{\rm nlcc}$. For this smoothly truncated core density, $n_{c,{\rm ps}}$ we have used the form[14]

$$n_{c,{\rm ps}}(r)=\begin{cases} n_0+\sum_{i=3}^{6} n_i r^i & \text{for } r<r_{\rm nlcc}, \\ n_c(r) & \text{for } r\geqslant r_{\rm nlcc}, \end{cases} \tag{22}$$

requiring continuity of $n_{c,{\rm ps}}$ as well as its first four derivatives at $r_{\rm nlcc}$. The actual values of $r_{\rm nlcc}$, which have been chosen rather conservatively (for a detailed discussion of this issue, see Ref. 22), are given in Table I.

III. TECHNICAL DETAILS

A. Details of the pseudopotential construction

In order to allow for convergence studies, a series of PPs has been produced for all $3d$ elements, starting with the minimum valence space $3d4s$ and successively including the $3p$ and $3s$ electrons.[39] This implies that ultimately two s orbitals are included in the valence space. One can then choose between two states from which the s-PP can be constructed. Using the energetically lower s state, i.e., the $3s$ orbital, the pseudo $4s$ orbital is obtained as the second lowest state bound by the s-PP and thus exhibits one node. At first glance, one might expect this first excited pseudo-orbital to differ significantly from the AE $4s$ orbital. However, this is not the case, as can be seen from Fig. 1, in which these

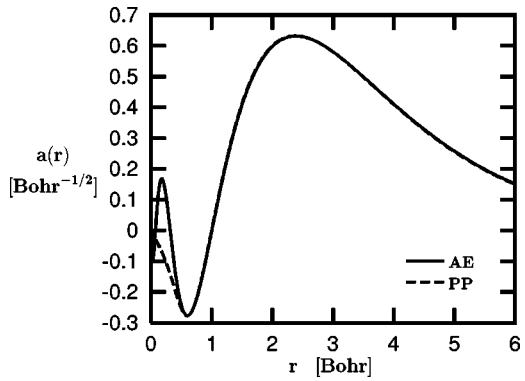

FIG. 1. Large component of 4*s* orbital of Fe. PO generated from 3*s*-PP in comparison with AE result.

two states are compared for Fe. The two 4*s* orbitals are almost indistinguishable in the valence regime. Correspondingly, the eigenvalue of the 4*s*-PO obtained from the 3*s*-PP is only marginally different from the AE 4*s*-eigenvalue (2 mHartree).

In spite of this very good agreement, the small differences between the two orbitals in the valence regime would lead to a minor mismatch between $v_{\mathrm{xc}}[n_{\mathrm{AE}}]$ and $v_{\mathrm{xc}}[n_{\mathrm{ps}}]$ if n_{ps} was evaluated with this 4*s*-PO. For maximum consistency we have thus always used the 4*s*-PO generated directly from the AE 4*s*-orbital in the unscreening procedure. To construct this 4*s*-PO, one has to choose $r_{c,s}$ somewhere in between the two outermost nodes of the AE 4*s*-orbital, so that the pseudo 4*s* state again has one node.[40]

Analogous statements hold for 4*d* and 5*d* elements. Quite generally, it seems that it is slightly preferable to use the higher state for the generation of the PP, as the corresponding PO is more important for the poly-atomic electronic structure. While we have found essentially no difference in the molecular results obtained with the two *s*-PP for the 3*d* elements, use of the PP generated from the 6*s*-state yields spectroscopic parameters for Au_2, which are marginally closer to the AE-data (the results of Tables VIII and IX correspond to this PP).

Rather hard cutoff radii have been used for this conceptual study, in order to avoid any inaccuracies, which could result from a softer choice for these input parameters (see Table I). The sensitivity of the molecular results to the cutoff radii chosen has been checked in detail for the various states of FeO, using the 3*p*3*d*4*s* valence space for Fe. Our standard r_c's for this configuration are 0.8 Bohr for the *p*- and *d*-PPs and 2.2 Bohr for the *s*-PP. Increasing the 3*p* cutoff radius from 0.8 to 1.6 Bohr, both the bond length and the harmonic frequency remain essentially invariant, while the binding energy is reduced by 0.05 eV. Differences of the same size are found between $r_{c,s}=2.2$ Bohr and $r_{c,s}=2.7$ Bohr. Consequently, the spectroscopic parameters are rather insensitive to variation of the 3*p* and 4*s* cutoff radii. The 3*d* cutoff radius, however, must not be increased beyond 0.9 Bohr if one wants to keep the resulting equilibrium distance within 0.1 Bohr of that found with the more accurate hard PP (i.e., for $r_{c,d}=0.8$ Bohr). On the other hand, further reduction of $r_{c,d}$ to 0.6 Bohr does not change any of the spectroscopic constants.

B. Details of the molecular calculations

For the molecular PP calculations, we have used prolate-elliptic coordinates and a Hylleraas-type basis. For the technical details of this nonrelativistic spin-density functional approach, the reader is referred to Ref. 41. Taking all technical sources of inaccuracies (basis sets, grids, etc.) together, the resulting equilibrium bond lengths (R_e) are converged to better than 0.01 Bohr, while dissociation energies (D_e) are correct within 0.01 eV and vibrational frequencies (ω_e) within 10 cm^{-1} (for given PP).

Our AE calculations for FeO have been performed with the Amsterdam code.[42] High quality triple zeta basis sets have been used for both Fe and O. For oxygen, an additional polarization function has been included.

In the case of open-shell atoms, the atomic ground state energy used for the evaluation of D_e needs some further specification in order to allow for unambiguous comparisons. Quite generally, both the exact ground state density and the density, which minimizes the LDA ground state energy functional, are nonspherical for this class of atoms (for a detailed discussion see Ref. 43). Moreover, nonspherical atomic ground state densities often lead to binding energies which are closer to the experimental values.[44] On the other hand, many calculations in the literature are based on atomic reference energies that correspond to spherically symmetric densities. In this work, we have thus restricted the atomic PP calculations for Fe, Ni, and O to spherical densities, in order to be consistent with the evaluation of the nonrelativistic AE reference values for D_e.[25,42]

It seems worth mentioning that the use of nonspherical atomic densities appears to be problematic for PP calculations without nlccs. For instance, the AE ground state energy of oxygen obtained with a nonspherical potential is 0.106 eV lower than that found with a spherical density (see Table II—in our calculations, a nonspherical density always implies a nonspherical total potential). While this energy gain is well reproduced by the PP calculation with nlccs (0.107 eV), it is clearly overestimated without nlccs (0.163 eV). As Table II shows, the effect can be similarly large even in the case of extended valence spaces. For Fe one finds an energy gain of 0.079 eV without nlccs for the *L* shell, 0.027 eV with nlccs. This overestimation introduces a systematic error in the corresponding D_e obtained from PP calculations without nlccs (compare Ref. 22).

IV. RESULTS

A. Role of semicore states

In this section we examine the convergence of molecular results for transition metal compounds with respect to the size of the valence space and, in particular, to what extent nlccs can substitute the explicit dynamic treatment of semicore states. As this question is not intimately linked to the relativistic approach and only nonrelativistic AE reference

TABLE II. Atomic ground state energies. Role of nonspherical density[34] (all calculations are strictly nonrelativistic).

Atom	Mode	spin ↑	spin ↓	$-E_{\mathrm{tot}}$ [Hartree]
O	AE	$2s2p^3$	$2s2p^1$	74.52741
O	AE	$2\sigma 1\pi^2 3\sigma$	$2\sigma 3\sigma$	74.53129
O	PP	$2s2p^3$	$2s2p^1$	15.80945
O	PP	$2\sigma 1\pi^2 3\sigma$	$2\sigma 3\sigma$	15.81543
O	PP	$2s2p^3$+nlcc	$2s2p^1$+nlcc	18.73802
O	PP	$2\sigma 1\pi^2 3\sigma$+nlcc	$2\sigma 3\sigma$+nlcc	18.74196
Fe	PP	$3s3p^3 3d^5 4s$	$3s3p^3 3d^1 4s$	122.99089
Fe	PP	$4\sigma 2\pi^2 5\sigma 1\delta^2 6\sigma 3\pi^2 7\sigma$	$4\sigma 2\pi^2 5\sigma 6\sigma 3\pi^1$	122.99379
Fe	PP	$3s3p^3 3d^5 4s$+nlcc	$3s3p^3 3d^1 4s$+nlcc	144.66126
Fe	PP	$4\sigma 2\pi^2 5\sigma 1\delta^2 6\sigma 3\pi^2 7\sigma$+nlcc	$4\sigma 2\pi^2 5\sigma 6\sigma 3\pi^1$+nlcc	144.66226

data[45] are available, all PP results of Sec. IV A are strictly nonrelativistic. The spectroscopic constants obtained with the various PPs for four prototype molecules are summarized in Tables III and IV. We start the discussion by an analysis of the $^7\Delta$ ground state of Fe_2, the observations being characteristic of all other states considered.

Focusing first on the data obtained without nlccs, it is obvious from Table III that the minimum valence space $3d4s$ is completely inadequate (as is well known). The inclusion of the $3p$ electrons in the valence space drastically improves D_e; however, at the same time it even worsens the agreement of R_e with the AE reference value. On the other hand, when going from the $3p3d4s$-PP to the $3s3p3d4s$ configuration, R_e is reduced by 0.1 Bohr. As neither the mere overlap of the $3s$ with the $3d$ orbital nor the polarization of the $3s$ density can be responsible for this effect (otherwise the differences between the minimum-PP and the $3p3d4s$-PP had to be larger), this indicates that the outermost node of the $4s$-orbital has some relevance for the molecular electronic structure. This node is located at 1.04 Bohr, i.e., even beyond the region where the $3d$ orbitals and the semicore density have their maxima, so that this manifestation of the orthogonality between the $4s$ and the $3s$ state can actually affect the molecular results.

This conclusion is confirmed by the spectroscopic constants found with nlccs. Even for the minimum valence space the $3s$ density is now taken into account, while the $4s$ node is still suppressed. As Table III shows, D_e is always significantly improved by the inclusion of nlccs. However, the same is not true for R_e and ω_e. On the one hand, the nlccs reduce the error in R_e by 40%, in the case of the minimum valence space. On the other hand, the $3p3d4s$ valence space shows that this improvement must be regarded as fortuitous. For this configuration the inclusion of nlccs does not affect R_e at all, so that the optimum PP without a dynamic treatment of the $3s$ electrons overestimates R_e by 0.1 Bohr. In other words, if nlccs are used the dynamic handling of the $3p$ electrons yields worse results than their representation via nlccs. Finally, for the $3s3p3d4s$ valence space the PPs with and without nlccs again give the same value for R_e (and ω_e).

Comparing the results from the largest valence space with the AE data,[25] one finds perfect agreement for R_e, indicating convergence of the PP approach. On the other hand, the D_e obtained with the PP without nlccs is still in error by almost 0.5 eV. In view of the very small core, this discrepancy is somewhat surprising. It can, however, be traced to the nonlinearity of $E_{\mathrm{xc}}[n]$. Even the xc-interaction of the semicore

TABLE III. Bond length R_e, dissociation energy D_e (including zero-point energy) and harmonic frequency ω_e of transition metal dimers: Nonrelativistic PP versus AE calculations.[34]

	Mode	PP valence configuration		R_e [Bohr]	D_e [eV]	ω_e [cm^{-1}]
Fe_2	PP	$3d^6 4s^2$		3.75	0.76	422
$^7\Delta$	PP	$3d^6 4s^2$	+nlcc	3.72	4.09	426
	PP	$3p^6 3d^6 4s^2$		3.78	3.40	452
	PP	$3p^6 3d^6 4s^2$	+nlcc	3.78	4.18	450
	PP	$3s^2 3p^6 3d^6 4s^2$		3.68	3.91	440
	PP	$3s^2 3p^6 3d^6 4s^2$	+nlcc	3.68	4.31	440
	AE[25]			3.68	4.38	497
	PP[1]	$3d^7 4s^1$	+nlcc	3.61	3.94	400
	PP[21]	$3s^2 3p^6 3d^6 4s^2$		3.70	4.12	
Ni_2	PP	$3d^8 4s^2$		3.86	3.93	367
$^3\Sigma$	PP	$3d^8 4s^2$	+nlcc	3.89	3.42	363
	PP	$3p^6 3d^8 4s^2$		3.89	3.54	372
	PP	$3p^6 3d^8 4s^2$	+nlcc	3.90	3.41	370
	PP	$3s^2 3p^6 3d^8 4s^2$		3.85	3.56	363
	PP	$3s^2 3p^6 3d^8 4s^2$	+nlcc	3.85	3.49	362
	AE[25]			3.87	3.64	354

TABLE IV. Same as Table III for transition metal oxides.

	Mode	PP valence configuration		R_e [Bohr]	D_e [eV]	ω_e [cm^{-1}]
FeO	PP	$3d^64s^2$		3.11	5.06	852
$^5\Delta$	PP	$3d^64s^2$	+nlcc	3.05	6.60	956
	PP	$3p^63d^64s^2$		3.07	6.12	960
	PP	$3p^63d^64s^2$	+nlcc	3.07	6.62	974
	PP	$3s^23p^63d^64s^2$		2.99	6.65	962
	PP	$3s^23p^63d^64s^2$	+nlcc	2.99	7.00	968
	AE			3.01	7.06	957
FeO	PP	$3d^64s^2$		3.10	6.38	953
$^5\Sigma$	PP	$3d^64s^2$	+nlcc	3.11	6.46	939
	PP	$3p^63d^64s^2$		3.12	6.28	959
	PP	$3p^63d^64s^2$	+nlcc	3.12	6.50	955
	PP	$3s^23p^63d^64s^2$		3.04	6.45	948
	PP	$3s^23p^63d^64s^2$	+nlcc	3.04	6.60	947
	AE			3.06	6.70	942
FeO	PP	$3d^64s^2$		3.17	6.40	921
$^7\Sigma$	PP	$3d^64s^2$	+nlcc	3.19	5.77	886
	PP	$3p^63d^64s^2$		3.19	5.72	902
	PP	$3p^63d^64s^2$	+nlcc	3.19	5.75	895
	PP	$3s^23p^63d^64s^2$		3.13	5.88	881
	PP	$3s^23p^63d^64s^2$	+nlcc	3.13	5.95	876
	AE			3.15	5.99	877
CrO	PP	$3d^54s^1$		3.27	4.42	719
$^5\Pi$	PP	$3d^54s^1$	+nlcc	3.11	5.77	926
	PP	$3p^63d^54s^1$		3.16	5.40	917
	PP	$3p^63d^54s^1$	+nlcc	3.13	5.85	967
	PP	$3s^23p^63d^54s^1$		3.01	6.06	952
	PP	$3s^23p^63d^54s^1$	+nlcc	2.99	6.38	978
	AE[51]			3.02	6.15	976

with the core states shows up in D_e, particularly for high spin states. This is immediately clear from the corresponding PP with nlccs. The resulting D_e is almost on top of the AE energy. Thus, for a fully quantitative reproduction of the AE structure and energetics of iron compounds, the combination of a large valence space and nlccs is required.

For further support of this conclusion, the results from two PP-calculations in the literature[1,21] are listed in Table III. On the basis of ultra-soft PPs (Ref. 46) for the $3d$ and $4s$ orbitals and nlccs for both semicore states R_e is underestimated by 0.07 Bohr and ω_e by 97 cm^{-1}. On the other hand, use of ultra-soft PPs for all relevant valence and semicore states[21] yields results which are much closer to the present and the AE data.

The picture sketched by the results for Fe_2 is confirmed by all other transition metal compounds considered here. In particular, the reduction of R_e by the dynamic treatment of the $3s$ electrons is present for all molecules. While for FeO it is of the same size as for Fe_2, it is even larger for CrO (see Table IV). For Ni_2, on the other hand, both the faster convergence, with respect to the size of the valence space, and the reduced effect of nlccs indicate that the semicore states and thus also the nodal structure of the $4s$ orbital are not as important as for Fe_2 (see Table III). It is nevertheless worth noting that in the case of Ni_2, the inclusion of the semicore states into the $3d4s$-PP via nlccs even leads to an increase of R_e, while their dynamic treatment reduces the bond length. The same feature is found for the $^5\Sigma$ and $^7\Sigma$ states of FeO.

TABLE V. Low-lying excitation energies of FeO. Nonrelativistic AE versus PP results.[34]

Mode	PP valence configuration		$^5\Delta \rightarrow {}^5\Sigma$ [eV]	$^5\Sigma \rightarrow {}^7\Sigma$ [eV]
PP	$3d^64s^2$		−1.32	−0.02
PP	$3d^64s^2$	+nlcc	0.14	0.69
PP	$3p^63d^64s^2$		−0.16	0.56
PP	$3p^63d^64s^2$	+nlcc	0.12	0.75
PP	$3s^23p^63d^64s^2$		0.20	0.57
PP	$3s^23p^63d^64s^2$	+nlcc	0.40	0.65
AE			0.36	0.71

In the case of FeO, the energy gaps between the three low-lying states $^5\Delta$, $^5\Sigma$, and $^7\Sigma$ provide a further quality criterion for the PPs. As different spin states are involved, the size of the excitation energies also indicates how well the magnetization of the corresponding bulk material can be reproduced. As Table V demonstrates, the $3d4s$-PP without nlccs suggests the $^7\Sigma$ to be the ground state, the $3p3d4s$ PP without nlccs the $^5\Sigma$, both results being in contradiction to the AE calculation (and experiment). Also, the standard PP for Fe (minimum valence space plus nlccs) does not give realistic energy gaps. Even in the case of the largest valence space, nlccs are required for an accurate description of the subtle energy balance between the $^5\Delta$ ground state and the $^5\Sigma$ first excited state.

Another quantity that offers itself for a comparison is the static electric dipole moment. The corresponding AE and PP data for the $^5\Delta$ state of FeO are listed in Table VI for a number of R-values. Given the sensitivity of the dipole moment to the basis set size, the agreement of the $3s3p3d4s$-PP values with the AE numbers over the complete range of R is excellent. At the experimental equilibrium distance of 3.06 Bohr the predicted moments are 4.462 Debye in the case of the AE and 4.486 Debye for the PP calculation. On the other hand, the $3d4s$-PP with nlccs is systematically off by almost 0.3 Debye.

TABLE VI. Dipole moment (in Debye) for the $^5\Delta$ state of FeO. Nonrelativistic AE versus PP results for various internuclear distances R.

R [Bohr]	AE	PP	
		$3s^23p^63d^64s^2$	$3d^64s^2$+nlcc
2.90	3.92	3.93	3.66
3.00	4.27	4.29	4.03
3.10	4.59	4.61	4.37

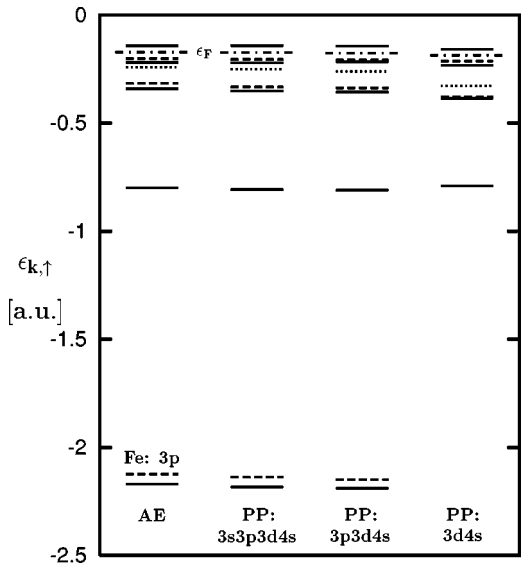

FIG. 2. Nonrelativistic spin-up eigenvalues of FeO (for $R=3.0$ Bohr). Various PPs without nlccs in comparison with AE result (σ-levels—solid lines, π-levels—dashed lines, δ-levels—dotted lines).

A more microscopic measure of the performance of PPs are the molecular KS eigenvalues. The spin-up single-particle spectra of FeO corresponding to the various PPs are compared with the AE-spectrum in Fig. 2. In accordance with the quality of the spectroscopic parameters, the eigenvalues of the $3d4s$-PP are clearly different from their AE-counterparts. In particular, the 1δ-level is bound too strongly. The $3p3d4s$-PP leads to a substantial improvement. The only obvious discrepancy to the AE spectrum is the underestimation of the splitting between the 8σ and the 4π level and the corresponding overestimation of the gap between the 8σ and the 1δ. Finally, the $3s3p3d4s$-PP produces a spectrum that agrees rather well with the AE-eigenvalues, in accordance with the quality of the spectroscopic data.

All these findings are in line with the results for atomic excitation energies (compare[1,22,47]). For Fe, all PPs without nlccs give completely inadequate values for the $^5D(3d^64s^2)\rightarrow{}^5F(3d^74s^1)$ excitation energy, as can be gleaned from Table VII.[48] Even the $3s3p3d4s$-PP overestimates the AE number by roughly a factor of 3. Inclusion of nlccs in this PP, on the other hand, leads to a s-d transfer energy reasonably close to the AE value. The improvement by nlccs is much less dramatic for Ni. Moreover, while the absolute errors of the optimum PPs are similar for both atoms (60–70 meV), the percentage error is 45% in the case of the very small s-d transfer energy of Fe, but only 4% for Ni. Among the elements listed in Table VII, Fe is clearly most sensitive to the handling of the semicore and core states.

For completeness we also list the spectroscopic constants of three noble metal compounds in Table VIII. One notes that even the minimum valence space ($(n-1)d^{10}ns^1$) without nlccs gives rather accurate results in the case of these

TABLE VIII. Same as Table III for noble metal compounds.

	Mode	PP valence configuration		R_e [Bohr]	D_e [eV]	ω_e [cm^{-1}]
Cu_2	PP	$3d^{10}4s^1$		4.14	2.58	268
$^1\Sigma$	PP	$3d^{10}4s^1$	+nlcc	4.14	2.58	281
	PP	$3p^63d^{10}4s^1$		4.14	2.59	286
	PP	$3p^63d^{10}4s^1$	+nlcc	4.14	2.59	286
	PP	$3s^23p^63d^{10}4s^1$		4.10	2.65	286
	PP	$3s^23p^63d^{10}4s^1$	+nlcc	4.10	2.65	286
	AE[10]			4.10	2.65	330
Au_2	PP	$5d^{10}6s^1$		5.10	1.98	136
$^1\Sigma$	PP	$5d^{10}6s^1$	+nlcc	5.11	1.98	135
	PP	$5p^65d^{10}6s^1$		5.11	1.99	138
	PP	$5p^65d^{10}6s^1$	+nlcc	5.11	1.98	138
	PP	$5s^25p^65d^{10}6s^1$		5.04	2.04	136
	PP	$5s^25p^65d^{10}6s^1$	+nlcc	5.04	2.04	136
	AE[11]			5.08	1.95	135
AuH	PP	$5d^{10}6s^1$		3.21	2.68	1704
$^1\Sigma$	PP	$5d^{10}6s^1$	+nlcc	3.20	2.69	1704
	PP	$5p^65d^{10}6s^1$		3.24	2.62	1693
	PP	$5p^65d^{10}6s^1$	+nlcc	3.25	2.62	1692
	PP	$5s^25p^65d^{10}6s^1$		3.21	2.68	1704
	PP	$5s^25p^65d^{10}6s^1$	+nlcc	3.21	2.69	1704
	AE[11]			3.21	2.63	1728

TABLE VII. $3d^n4s^2\rightarrow3d^{n+1}4s^1$ excitation energy: Nonrelativistic AE versus PP results.[34]

PP valence configuration		$E_{tot}(3d^{n+1}4s^1)-E_{tot}(3d^n4s^2)$ [eV] Cr	Mn	Fe	Co	Ni
$3d^n4s^m$		−2.950	4.170	2.361	0.692	−0.785
$3p^63d^n4s^m$		−2.234	1.735	0.702	−0.324	−1.327
$3s^23p^63d^n4s^m$		−2.090	1.379	0.445	−0.490	−1.410
$3d^n4s^m$	+nlcc	−2.146	1.202	0.311	−0.584	−1.447
$3p^63d^n4s^m$	+nlcc	−2.086	1.109	0.229	−0.656	−1.513
$3s^23p^63d^n4s^m$	+nlcc	−2.020	1.082	0.212	−0.666	−1.512
AE		−2.060	1.026	0.146	−0.721	−1.573

TABLE IX. Spectroscopic constants of noble metal compounds: Relativistic PP versus AE calculations.[34] IPP corresponds to a partially relativistic PP (see text).

	Mode	PP valence configuration		R_e [Bohr]	D_e [eV]	ω_e [cm^{-1}]
Cu_2	IPP	$3d^{10}4s^1$		3.66	3.78	474
$^1\Sigma$	IPP	$3p^63d^{10}4s^1$		3.94	3.42	338
	IPP	$3s^23p^63d^{10}4s^1$		3.85	4.07	349
	RPP	$3d^{10}4s^1$		4.07	2.74	298
	RPP	$3p^63d^{10}4s^1$		4.08	2.76	304
	RPP	$3s^23p^63d^{10}4s^1$		4.04	2.83	304
	RAE[12]			4.05	2.85	306
	Expt.[52]			4.20	2.05	265
Au_2	RPP	$5s^25p^65d^{10}6s^1$		4.60	3.04	198
$^1\Sigma$	RPP	$5s^25p^65d^{10}6s^1$	$+5f^0$	4.61	3.02	198
	RAE[16]			4.64	3.00	196
	Expt.[52]			4.67	2.30	191
AuH	RPP	$5s^25p^65d^{10}6s^1$		2.87	3.86	2341
$^1\Sigma$	RAE[12]			2.89	3.78	2339
	Expt.[52]			2.87	3.35	2305

elements. This shows that the spatial overlap between the $3d$ and $3p$ orbitals is only of minor importance for Cu and Au, so that nlccs can be safely neglected. Nevertheless, it seems worth pointing out that again the dynamic treatment of the $(n-1)s$ electrons is required to obtain the correct bond lengths (in the case of Au_2, we believe that the discrepancy between PP and AE data is due to the use of an insufficient basis set in Ref. 11—compare the relativistic values of Sec. IV B).

B. Importance of relativistic corrections

The discussion of Sec. IV A has set the stage for an analysis of the role of relativity for $3d$ compounds. The spectroscopic constants obtained with the relativistic TM PPs are summarized in Tables IX and X. We first analyze the results for the noble metal molecules listed in Table IX. For these systems, accurate relativistic AE results are available in the literature,[12,16] so that they are ideally suited for analyzing the performance of the relativistic TM PPs. In order to emphasize the importance of a consistent relativistic PP construction, we first reexamine the convergence of the PP results with decreasing size of the core for Cu_2. Two sets of PPs are compared. On the one hand, the consistent relativistic PPs developed in Sec. II A show a completely analogous behavior as their nonrelativistic limits. They converge in a similar manner and the $3s3p3d4s$-PP reproduces the relativistic AE data very well. On the other hand, we give the spectroscopic parameters obtained with a PP based on a partially nonrelativistic TM scheme. This ''inconsistent'' PP (IPP) results from an unscreening of the PP (11) with POs obtained by solution of Eqs. (3) and (4) with this PP. As discussed in Sec. II, this leads to an incomplete cancellation of the interaction among the valence electrons, the effect being of the order $1/c^2$. As is obvious from Table IX, the corresponding molecular data are rather different from those of the consistent PPs. They neither converge systematically with the size of the valence configuration nor are they close to the AE values. The particular sensitivity of the molecular results to an accurate unscreening does not allow for inconsistencies of the order $1/c^2$.

TABLE X. Same as Table IX for transition metal compounds.

	Mode	PP valence configuration		R_e [Bohr]	D_e [eV]	ω_e [cm^{-1}]
Fe_2	RPP	$3d^64s^2$	+nlcc	3.69	3.76	435
$^7\Delta$	RPP	$3s^23p^63d^64s^2$	+nlcc	3.66	3.95	451
	Expt.[53]			3.82	1.30	300
Ni_2	RPP	$3d^84s^2$	+nlcc	3.85	3.58	378
$^3\Sigma$	RPP	$3s^23p^63d^84s^2$	+nlcc	3.81	3.65	381
	Expt.[54]			4.07	2.07	330
FeO	RPP	$3d^64s^2$	+nlcc	3.03	6.45	972
$^5\Delta$	RPP	$3s^23p^63d^64s^2$	+nlcc	2.97	6.80	984
	Expt.[29,30]			3.06	4.06	881
$^5\Sigma$	RPP	$3d^64s^2$	+nlcc	3.09	6.44	956
	RPP	$3s^23p^63d^64s^2$	+nlcc	3.01	6.59	969
$^7\Sigma$	RPP	$3d^64s^2$	+nlcc	3.17	5.71	888
	RPP	$3s^23p^63d^64s^2$	+nlcc	3.12	5.88	884
CrO	RPP	$3d^54s^1$	+nlcc	3.10	5.92	940
$^5\Pi$	RPP	$3s^23p^63d^54s^1$	+nlcc	2.99	6.53	991
	Expt.[51]			3.05	4.41	898

Comparing the relativistic PP data to experiment, one observes the well-documented deficiencies of the LDA.[12] The LDA underestimates R_e for third row elements and clearly overestimates D_e. However, in the present context, the relevant reference data for the PP results are provided by an AE calculation using the same xc-functional, rather than by experiment. Of course, the PP cannot and should not correct for the errors of the LDA. The remaining discrepancies, with respect to experiment, can be accounted for by inclusion of gradient corrections in $E_{xc}[n]$,[12] and the present PP approach can be directly applied for such gradient corrected functionals.

In order to test the performance of the relativistic PP in the high-Z regime we have studied Au_2 and AuH: gold compounds reflect the ''gold maximum''[13] of relativistic effects observed in the periodic table. As Table IX shows, the agreement of the $5s5p5d6s$-PP results with their AE counterparts[12,16] is very satisfying, taking into account the enhanced importance of basis set limitations (in the case of AuH, the AE data correspond to a weakly relativistic calculation[12]). While our results are stable against variation of basis and grid sizes on the 0.01 Bohr and 0.01 eV level,

the convergence study of Liu and van Wüllen,[16] with respect to their AE basis set size, seems to indicate that the true AE bond length of Au_2 is somewhat shorter than the value of 4.64 Bohr obtained with their largest basis set. In addition, their AE dissociation energy seems to approach a value slightly larger than 3.00 eV, so that fully converged AE results should be even closer to our PP data.

We have also checked the effect of an *f*-component in the PP for Au. Following the procedures of both Bachelet *et al.*[7] (using Au^{2+} and a partial occupation of the $5f$-state in order to make the $5f$ state bound within the LDA) and Hamann[49] (using the $6s$-eigenvalue as orbital energy for the *f*-state), two different *f*-PPs have been constructed. Consistently, inclusion of either form of the *f*-PP led to an increase of the bond length of Au_2 by 0.01 Bohr and a decrease of D_e by 0.02 eV. Omission of the *f*-component thus accounts for only a minor part of the difference between PP and AE data.

Tables VIII and IX directly allow to extract the relativistic corrections to the spectroscopic constants of the three molecules. As is well known, they are sizable even for Cu_2 and extremely important for the Gold compounds. In view of the accuracy of the individual converged PP values for R_e, D_e, and ω_e, it is clear that also the relativistic corrections are well reproduced by the PPs.

We now turn to the transition metal compounds (Tables X). For these molecules only two PP variants are given: the standard PP, combining the minimum valence space with nlccs, and the optimum PP ($3s3p3d4s$ valence space plus nlccs). We first concentrate on the latter in order to examine the role of relativity for these systems. For Fe_2, one observes a bond length reduction of 0.02 Bohr accompanied by a destabilization of the bond by 0.37 eV, when going from the nonrelativistic to the relativistic PP. For Ni_2, the bond length contraction increases to 0.04 Bohr, while the correction to D_e amounts to 0.16 eV.[50] Corrections of similar size are found for FeO and CrO. While relativistic corrections of this size might be irrelevant for many studies of transition metal compounds, they certainly cannot be neglected if one aims at a quantitative comparison with experiment. Moreover, as the example of FeO shows, relativity does not affect all molecular states in the same way. The relativistic corrections destabilize the ground state by 0.20 eV and the $^7\Sigma$ by 0.15 eV, but do not change the binding energy of the first excited state. As a consequence, the $^5\Delta$ state is only 0.20 eV below the $^5\Sigma$ in the relativistic case, and the $^5\Sigma$ is stabilized with respect to the $^7\Sigma$ (compare the nonrelativistic energy gaps given in Table V). In other words, for critical systems like the transition metal oxides, relativistic corrections can be of the same order of magnitude as the energy gaps between the low-lying states.

The importance of this observation becomes particularly obvious when looking at the relativistic version of the standard PP for Fe. This PP erroneously predicts the $^5\Delta$ to be degenerate with the $^5\Sigma$, which questions its suitability for transition metal oxides. Only the combination of a dynamic treatment of the semicore states and nlccs allows reliable PP calculations for this type of system.

Compared with the experimental data, the most advanced PP yields bond lengths which are too short by 0.06 (CrO) to 0.26 (Ni_2) Bohr and binding energies, which are too large by more than 2 eV. In their AE calculations Castro *et al.*[25] showed that for Fe_2 and Ni_2 one can bridge part of this gap by inclusion of gradient corrections. For instance, for Fe_2, the gradient terms increase R_e by 0.05 Bohr and decrease D_e by more than 1 eV. We expect an analogous behavior for the PP approach.

V. CONCLUDING REMARKS

In view of the consistent and accurate performance observed so far, the PP construction scheme presented in this paper offers itself as an extension of the standard TM procedure to all elements for which relativistic effects cannot be neglected. As our results show, proper account of relativity is not only pertinent for an understanding of the cohesive properties of very heavy elements. Relativistic corrections are also visible in the bond lengths and dissociation energies of all $3d$ compounds considered here. While contributions of 0.02–0.06 Bohr to R_e and 0.2–0.4 eV to D_e might not be relevant for all kinds of PP applications, they can nevertheless not be neglected if one aims at a fully quantitative description of the system, as is usually the case in GGA calculations. In fact, for all molecules in the present study the relativistic PPs lead to a contraction of R_e, thus acting in the opposite direction as the nonlocal (gradient) contributions to the xc-functional. The size of this contraction is not negligible compared with the bond stretching by the gradient term (0.02 vs 0.05 Bohr for Fe_2[25]). Moreover, for systems like FeO in which the first excited state is energetically close to the ground state, the relativistic corrections can substantially modify the energy gap between the two states. For instance, for the lowest excitation energy of FeO, one finds 0.20 eV with the relativistic approach, compared to the nonrelativistic value of 0.40 eV. It seems worth emphasizing that in its *j*-averaged form, the relativistic TM scheme allows for the inclusion of relativity in molecular or bulk calculations at essentially no cost, on the level of both the LDA and the GGA. Thus consistent use of the relativistic TM variant seems recommendable.

As a prerequisite for the discussion of relativistic corrections, we have analyzed the convergence of PP results with the size of the valence space. All our results suggest that for transition metal elements, the presence of the outermost node of the valence *s* state, i.e., the orthogonality of this state with the semicore *s* state, is important for the molecular electronic structure. In PP calculations, this node is suppressed as long as the semicore *s* state is taken into account via nlccs; only an explicit dynamic treatment of this state preserves the nodal structure. When going from the nlcc to the dynamic representation of the $3s$, the bond lengths reduce by 0.08–0.10 Bohr for the iron compounds, 0.14 Bohr for CrO, and 0.05 Bohr for Ni_2. Moreover, the nlcc representation predicts the $^5\Delta$ and $^5\Sigma$ states of FeO to be degenerate, in obvious contradiction to the more advanced calculations and to experiment. On the other hand, the converged PP, in which the semicore states are included in the valence space, gives results in excellent agreement with the AE calculation. As the observed limitations of the nlcc concept do not origi-

nate from specific features of the TM scheme, we believe them to apply also to other PP approaches. It thus seems that in PP calculations for transition metal elements, and especially for iron, the semicore electrons should be treated dynamically.

ACKNOWLEDGMENTS

We would like to thank R. Schmid for a careful reading of the manuscript. Financial support by the Studienstiftung des Deutschen Volkes (A.H.), the German Academic Exchange Service, DAAD (S.V.), and the Deutsche Forschungsgemeinschaft is gratefully acknowledged.

APPENDIX: CONTINUITY CONDITIONS FOR RELATIVISTIC PSEUDO-ORBITALS

As can be seen on the basis of the relativistic KS equation (12), the continuity of the PO and its first four derivatives at $r_{c,l}$ is ensured by

$$p=\ln\left(\frac{a}{r^{l+1}}\right), \tag{A1}$$

$$p'=\frac{a'}{a}-\frac{l+1}{r}, \tag{A2}$$

$$p''=2m(1-\Delta)(v-\epsilon)-p'^2-2\frac{l+1}{r}p'-\frac{\Delta'\alpha}{1-\Delta}, \tag{A3}$$

$$p'''=2m(1-\Delta)v'-2m\Delta'(v-\epsilon)-2p'p''+2\frac{l+1}{r^2}p' -2\frac{l+1}{r}p''-\frac{\Delta''\alpha}{1-\Delta}-\frac{(\Delta')^2\alpha}{(1-\Delta)^2}-\frac{\Delta'\alpha'}{1-\Delta}, \tag{A4}$$

$$p'''=2m(1-\Delta)v''-4m\Delta'v'-2m\Delta''(v-\epsilon)-2p'p''' -2(p'')^2-4\frac{l+1}{r^3}p'+4\frac{l+1}{r^2}p''-2\frac{l+1}{r}p''' -\frac{\Delta'''\alpha}{1-\Delta}-3\frac{\Delta'\Delta''\alpha}{(1-\Delta)^2}-2\frac{(\Delta')^3\alpha}{(1-\Delta)^3}-2\frac{\Delta''\alpha'}{1-\Delta} -2\frac{(\Delta')^2\alpha'}{(1-\Delta)^2}-\frac{\Delta'\alpha''}{1-\Delta}. \tag{A5}$$

Here a and v denote the AE orbital and potential at $r=r_{c,l}$ and $\alpha=p'+(l+1+\kappa)/r$. In addition to Eqs. (A1)–(A5) one usually requires the second derivative of $v_{\rm ps}^{\rm sc}$ to vanish at $r=0$. For the nonrelativistic part of $v_{\rm ps}^{\rm sc}$, the small r expansion reads

$$v_{\rm ps}^{\rm sc,nr}(r)=\epsilon+(2l+3)\frac{c_2}{m}+\frac{2}{m}[(2l+5)c_4+c_2^2]r^2+\cdots,$$

so that one obtains the condition[8]

$$c_4=-c_2^2/(2l+5). \tag{A6}$$

Given this relation, δv also vanishes for all states with $j=l+1/2$, while one finds a nonzero second derivative for $j=l-1/2$,

$$\delta v=\frac{1}{2m^3c^2}\{(2l+3)^2c_2^2+2(l+1+\kappa)[(2l+5)c_4+c_2^2] +[4(2l+4)c_2[(2l+5)c_4+c_2^2] +2(l+1+\kappa)[(6l+21)c_6+8c_2c_4]]r^2\}.$$

However, the nonzero contribution to $(v_{\rm ps}^{\rm sc})''$ at the origin is proportional to $1/c^2$, so that its actual size is small. Moreover, the unscreening procedure (14) also introduces a term proportional to r^2 in $v_{\rm ps}$, so that the size of $(v_{\rm ps}^{\rm sc})''$ at $r=0$ is not the only criterion relevant for the convergence of the Fourier expansion of the unscreened PP. We have thus used the nonrelativistic requirement (A6) in this work.

[1] E.G. Moroni, G. Kresse, J. Hafner, and J. Furthmüller, Phys. Rev. B **56**, 15 629 (1997).
[2] N. Chetty, M. Weinert, T.S. Rahman, and J.W. Davenport, Phys. Rev. B **52**, 6313 (1995).
[3] M. Krajci, J. Hafner, and M. Mihalkovic, Phys. Rev. B **56**, 3072 (1997); M. Krajci and J. Hafner, *ibid.* **58**, 5378 (1998).
[4] C.G. Morgan, P. Kratzer, and M. Scheffler, Phys. Rev. Lett. **82**, 4886 (1999).
[5] R.N. Barnett and U. Landman, Phys. Rev. B **48**, 2081 (1993).
[6] M. Eichinger, P. Tavan, J. Hutter, and M. Parinello, J. Chem. Phys. **110**, 10 452 (1999); D. Marx, M.E. Tuckerman, J. Hutter, and M. Parinello, Nature (London) **397**, 601 (1999).
[7] D.R. Hamann, M. Schlüter, and C. Chiang, Phys. Rev. Lett. **43**, 1494 (1979); G.B. Bachelet, D.R. Hamann, and M. Schlüter, Phys. Rev. B **26**, 4199 (1982).
[8] N. Troullier and J.L. Martins, Phys. Rev. B **43**, 1993 (1991).
[9] See, e.g., R. M. Dreizler and E. K. U. Gross, *Density Functional Theory* (Springer, Berlin, 1990).
[10] G.S. Painter and F.W. Averill, Phys. Rev. B **28**, 5536 (1983).
[11] C. van Wüllen, J. Chem. Phys. **103**, 3589 (1995).

[12] M. Mayer, O.D. Häberlen, and N. Rösch, Phys. Rev. A **54**, 4775 (1996).
[13] P. Pyykkö, Chem. Rev. **88**, 563 (1988).
[14] M. Fuchs and M. Scheffler, Comput. Phys. Commun. **119**, 67 (1999).
[15] M. Seth, P. Schwerdtfeger, and M. Dolg, J. Chem. Phys. **106**, 3623 (1996); F. Rakowitz, M. Casarrubios, L. Seijo, and C.M. Marian, *ibid.* **108**, 7980 (1998); G. Theurich and N. H. Hill, Phys. Rev. B (to be published).
[16] W. Liu and C. van Wüllen, J. Chem. Phys. **113**, 2506 (2000); **110**, 3730 (1999).
[17] S.G. Louie, S. Froyen, and M.L. Cohen, Phys. Rev. B **26**, 1738 (1982).
[18] J. Zhu, X.W. Wang, and S.G. Louie, Phys. Rev. B **45**, 8887 (1992).
[19] J.-H. Cho, and M. Scheffler, Phys. Rev. B **53**, 10 685 (1996).
[20] P. Ballone and R.O. Jones, Chem. Phys. Lett. **233**, 632 (1995).
[21] T. Oda, A. Pasquarello, and R. Car, Phys. Rev. Lett. **80**, 3622 (1998).
[22] D. Porezag, M.A. Pederson, and A.Y. Liu, Phys. Rev. B **60**, 14 132 (1999).
[23] M. Fuchs, M. Bockstedte, E. Pehlke, and M. Scheffler, Phys. Rev. B **57**, 2134 (1998).
[24] J.L. Chen, C.S. Wang, K.A. Jackson, and M.A. Pederson, Phys. Rev. B **44**, 6558 (1991).
[25] M. Castro and D.R. Salahub, Phys. Rev. B **49**, 11 842 (1994); M. Castro, C. Jamorski, and D.R. Salahub, Chem. Phys. Lett. **271**, 133 (1997).
[26] Z. Fang, I.V. Solovyev, H. Sawada, and K. Terakura, Phys. Rev. B **59**, 762 (1999).
[27] The use of nlccs is not possible in the case of truly nonlocal xc-functionals, like the exact exchange, so that one necessarily has to rely on linear unscreening for these DFT schemes.
[28] M. Krauss and W.J. Stevens, J. Chem. Phys. **82**, 5584 (1985).
[29] E. Murad, J. Chem. Phys. **73**, 1381 (1980).
[30] A.S.C. Cheung, R.M. Gordon, and A.J. Merer, J. Mol. Spectrosc. **87**, 289 (1981).
[31] S.H. Vosko, L. Wilk, and M. Nusair, Can. J. Phys. **58**, 1200 (1980).
[32] D.M. Bylander and L. Kleinman, Phys. Rev. Lett. **74**, 3660 (1995); Phys. Rev. B **52**, 14 566 (1995); **54**, 7891 (1996); **55**, 9432 (1997); M. Städele, J.A. Majewski, P. Vogl, and A. Görling, Phys. Rev. Lett. **79**, 2089 (1997); M. Städele, M. Moukara, J.A. Majewski, P. Vogl, and A. Görling, Phys. Rev. B **59**, 10 031 (1999); A. Höck and E. Engel, Phys. Rev. A **58**, 3578 (1998).
[33] E. Engel and R.M. Dreizler, J. Comput. Chem. **20**, 31 (1999).
[34] For v_{loc}, we have always used the *s*-PP in the case of the transition and noble metal elements, while the *p*-PP has been utilized for oxygen.
[35] The importance of the AE valence configuration has been examined for Fe. In the case of the largest valence space, absolutely no differences were found between the spectroscopic constants obtained with the $3d^6 4s^2$ ground state and those resulting from the $3d^7 4s^1$ configuration for all molecules and states considered. For the minimum valence space, the differences are somewhat larger, but use of the $3d^7 4s^1$ configuration did not lead to a systematic improvement. While the binding energy of Fe_2 becomes more accurate, the R_e of all states of FeO become worse.
[36] E. Engel, A. Facco Bonetti, S. Keller, I. Andrejkovics, and R.M. Dreizler, Phys. Rev. A **58**, 964 (1998).
[37] M.E. Rose, *Elementary Theory of Angular Momentum* (Wiley, New York, 1957).
[38] The proportionality of $a_{ps,lj}$ to r^{l+1} for small r represents the correct r-dependence required by Eqs. (3) and (4) for a potential which remains finite at $r=0$ (as the PP).
[39] In the case of the minimum configuration, the *p*-PP has been obtained from the unoccupied $4p$-orbital, which is bound within the LDA for all the atoms considered here.
[40] The resulting *s*-PP then has a nodeless eigenstate that is energetically lower than the $4s$-level. For $r>r_{c,s}$ this pseudo-$3s$-orbital is very close to the corresponding AE orbital.
[41] E. Engel, A. Höck, and R.M. Dreizler, Phys. Rev. A **62**, 042502 (2000).
[42] ADF 2.3.0, Theoretical Chemistry, Vrije Universiteit, Amsterdam, E.J. Baerends *et al.*, Chem. Phys. **2**, 41 (1973); G. te Velde and E.J. Baerends, J. Comput. Phys. **99**, 84 (1992); C. Fonseca Guerra, O. Visser, J.G. Snijders, G. te Velde, and E.J. Baerends, in *METECC95 - Methods and Techniques in Computational Chemistry*, edited by E. Clementi and G. Corongiu (STEF, Cagliar, 1995), p. 305.
[43] H.A. Fertig and W. Kohn, Phys. Rev. A **62**, 052511 (2000).
[44] F.W. Kutzler and G.S. Painter, Phys. Rev. Lett. **59**, 1285 (1987).
[45] For an unambiguous comparison between AE and PP results, it is important that the same xc-functional is used in both calculations. The differences originating from use of two different $E_{\mathrm{xc}}[n]$ can be of the same order of magnitude as those found for two different PPs (or even larger).
[46] D. Vanderbilt, Phys. Rev. B **41**, R7892 (1990).
[47] O. Gunnarsson and R.O. Jones, Phys. Rev. B **31**, 7588 (1985); J.B. Lagowski and S.H. Vosko, Phys. Rev. A **39**, 4972 (1989).
[48] The energies in Table VII have been obtained with a finite differences code, restricting the density to be spherical, so that basis set incompleteness does not affect these results.
[49] D.R. Hamann, Phys. Rev. B **40**, 2980 (1989).
[50] Although the relativistic corrections are only two to three times as large as the absolute accuracy of D_e, we believe them to be rather accurate as they result from two PPs whose construction only differs in the handling of relativity.
[51] S. Veliah, K. Xiang, R. Pandey, J.M. Recio, and J.M. Newsam, J. Chem. Phys. **102**, 1126 (1998).
[52] K. P. Huber and G. L. Herzberg, *Molecular Spectra and Molecular Structure. IV. Constants of Diatomic Molecules* (Van Nostrand Reinhold, New York, 1979).
[53] H. Purdum, P.A. Montana, G.K. Shenoy, and T. Morrison, Phys. Rev. B **25**, 4412 (1982); M. Moskovits, D.P. DiLella, and W. Limm, J. Chem. Phys. **80**, 626 (1984); M. Moskovits and D.P. DiLella, *ibid.* **73**, 4917 (1980).
[54] M.D. Morse, G.P. Hansen, P.R.R. Langridge-Smith, L.-S. Zheng, M.E. Geusic, D.L. Michalopoulos, and R.E. Smalley, J. Chem. Phys. **80**, 5400 (1984); M. Moskovits and J.E. Hulse, *ibid.* **66**, 3988 (1977).